

Enhancing quantum entanglement and quantum teleportation for two-mode squeezed vacuum state by local quantum-optical catalysis

Xue-xiang Xu

Department of Physics, Jiangxi Normal University,
Nanchang 330022, China;

[†]Corresponding author: xxxjxnu@gmail.com

I investigate how the entanglement properties of a two-mode squeezed vacuum state (TMSVS) can be enhanced by operating quantum-optical catalysis, proposed by Lovvky and Mlynek [Phys. Rev. Lett. 88, 250404 (2002)], on each mode. I show that the degree of entanglement, the Eistein-Podolsky-Rosen-type correlation, and the performance of quantum teleportation can be all enhanced for the output state when the appropriate quantum-optical catalysis is applied to a TMSVS. It is found that all the enhancements are happened in the small-squeezing and small-catalysis parameter regime.

PACS: 03.67.-a, 05.30.-d, 42.50.Dv, 03.65.Wj

Keywords: Degree of entanglement; EPR correlation; Teleportation fidelity; Quantum-optical catalysis

I. INTRODUCTION

Entangled resources are useful in quantum information processing, such as quantum teleportation[1], metrology[2] and communications[3]. In the continuous-variable (CV) regime, two-mode Gaussian entangled states, such as two-mode squeezed vacuum states (TMSVSs), are typically employed as entangled resources[4–6]. However, theoretical investigations have shown that Gaussian entangled resources have some restrictions[7, 8]. For example, entanglement distillation from two Gaussian entangled state is impossible by Gaussian local operations and classical communication[9, 10]. Therefore, it is desirable to seek non-Gaussian entangled resources and operations which can be more efficient in the quantum information processing. In recent years, some entanglement criteria beyond the Gaussian regime, including all orders of EPR correlations, have been proposed[11, 12]. Moreover, it has been shown that non-Gaussian two-mode entangled states provide the benefits of enhancing the entanglement[13–16].

Previously, the effect of entanglement has been theoretically analyzed based on the merit of concrete protocol, such as the degree of entanglement, the EPR correlation and the fidelity of teleportation[13, 14]. In fact, it was shown that the performance of every protocol was improved, implying that the entanglement of a non-Gaussian state must be enhanced[12]. In recent years, many schemes of generating two-mode non-Gaussian entangled states have been proposed. Among these schemes, performing non-Gaussian operation on a two-mode Gaussian state is one possible approach to generate non-Gaussian entangled resources[17, 18]. These typical non-Gaussian operations include the elementary operations (i.e. photon addition a^\dagger, b^\dagger and subtraction a, b) and their sequential operations (e.g. $ab, a^\dagger b^\dagger$)[19, 20] as well as their coherent superposition (e.g. $a^{\dagger 2} + b^{\dagger 2}$)[21]. Recently, for implement multiple photon addition and subtraction on both modes of the TMSVS, Navarrete-

Benloch et al [15] demonstrate that the entanglement generally increases with the number of such operations. On the other hand, one can generate non-Gaussian entangled resources by means of linear or nonlinear quantum optical system[22–24]. The systems generally consist of beam splitting, phase shifting, squeezing, displacement, and various detection.

About two decades ago, the concept of “conditional measurement” was proposed by Dakna et al[25]. They generate a Schrodinger-cat-like state by using a simple beam-splitter (BS) scheme for a conditional measurement. Following Dakna’s idea of conditional measurement, many schemes have been proposed to prepare quantum states[26–28]. Among these works, the typical proposal is the quantum-optical catalysis, proposed by Lovvky and Mlynek[29]. They generated a coherent superposition state $t|0\rangle + \alpha|1\rangle$ by conditional measurement on a BS. This state was generated in one of the BS output channels if a coherent state $|\alpha\rangle$ and a single-photon Fock state $|1\rangle$ are present in two input ports and a single photon is registered in the other BS output. They call this transformation “quantum-optical catalysis” because the single photon itself remains unaffected but facilitate the conversion of the target ensemble. Recently, Bartley et. al.[30] perform quantum-optical catalysis to generate multiphoton nonclassical states, which create a wide range of nonclassical phenomena. Since performing quantum-optical catalysis on a single-mode Gaussian state can enhance nonclassicality of the given state, one can ask if it is possible to enhance entanglement of a two-mode Gaussian state via quantum-optical catalysis. To my knowledge, this problem has not been perviously addressed.

In this paper, I propose a novel scheme to generate a two-mode non-Gaussian entangled state. This state is generated by operating quantum-optical catalysis on each mode of a TMSVS. I investigate the entanglement properties (the degree of entanglement and EPR correlation) and the quantum teleportation fidelity for the state I produce. I show that when ideal quantum-optical catal-

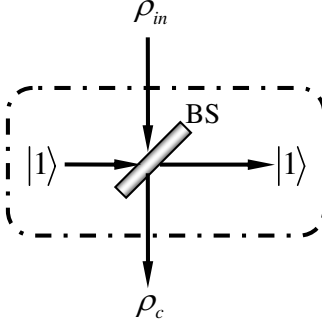


FIG. 1: (Color online) Basic block of the quantum-optical catalysis. An input state ρ_{in} and a single-photon Fock state $|1\rangle$ are present in the two input ports of the BS. Measurement is conditioned on registering a single photon $|1\rangle$ by the single-photon detector. Here the output state ρ_c is called as the catalysis state of the input state ρ_{in} and this process is quantum-optical catalysis. The catalysis parameter is the tunable transmissibility of the BS.

ysis is used, the input Gaussian state can be transformed into a non-Gaussian state with higher entanglement.

The paper is organized as follows. In section II, I begin with the generation of a non-Gaussian two-mode entangled state by operating quantum-optical catalysis from a two-mode squeezed vacuum state (TMSVS) and derive its normalization factor (i.e. success probability), which is important to discussing quantum properties. In section III, I investigate the entanglement properties (degree of entanglement and EPR correlation) of the non-Gaussian state and analyze the effect of the local quantum-optical catalysis. Then I consider the non-Gaussian entangled state as entangled resource to teleport a coherent state in section IV. The main results are summarized in Sec.V.

II. TWO-MODE NON-GAUSSIAN ENTANGLED STATE BY LOCAL QUANTUM-OPTICAL CATALYSIS

In this section, I apply quantum-optical catalysis to prepare a new two-mode non-Gaussian quantum state. The theoretical scheme is proposed and the success probability is derived.

A. Theoretical scheme

The basic idea on the quantum-optical catalysis was introduced in Ref. [29]. The conceptual schematic is shown in figure 1. If an input state ρ_{in} and a single-photon Fock state $|1\rangle$ are present in the two input ports of the BS and a single photon $|1\rangle$ is registered in one BS output port, then a catalyzed state ρ_c can be generated in the other BS output channel.

My scheme is depicted in Fig.2. Theoretically, the input TMSVS $|\psi_0\rangle_{ab}$ is obtained by applying the unitary operator $S_2(r)$ on the two-mode vacuum $|0_a, 0_b\rangle$, i.e.

$$\begin{aligned} |\psi_0\rangle_{ab} &= S_2(r) |0_a, 0_b\rangle \\ &= \frac{1}{\cosh r} \exp(a^\dagger b^\dagger \tanh r) |0_a, 0_b\rangle \\ &= \frac{1}{\cosh r} \sum_{n=0}^{\infty} \tanh^n r |n_a, n_b\rangle, \end{aligned} \quad (1)$$

where $S_2(r) = \exp[r(a^\dagger b^\dagger - ab)]$ is the two-mode squeezed operator and the values of r determines the degree of squeezing. The larger r , the more the state is squeezed. In particularly, when $r = 0$, $|\psi_0\rangle_{ab}$ reduces to $|0_a, 0_b\rangle$. Enlighten by the idea of quantum-optical catalysis, I prepare a new state from the TMSVS $|\psi_0\rangle_{ab}$ by operating quantum-optical catalysis on each mode. Then the prepared state $|\psi_{LQC}\rangle_{ab}$ is given by

$$|\psi_{LQC}\rangle_{ab} = \frac{1}{\sqrt{p_{cd}}} \langle 1_d | \langle 1_c | B_2 B_1 S_2(r) |0_a, 0_b\rangle |1_c\rangle |1_d\rangle, \quad (2)$$

which I call it ‘‘local quantum catalyzed TMSVS’’ (LQC-TMSVS). Here B_1 and B_2 corresponds to the respective unitary operators of the two tunable BS_1 and BS_2 ,

$$B_1 = \exp[\theta_1 (a^\dagger c - ac^\dagger)], \quad B_2 = \exp[\theta_2 (b^\dagger d - bd^\dagger)]. \quad (3)$$

in terms of the creation (annihilation) operator $a^\dagger(a)$, $b^\dagger(b)$, $c^\dagger(c)$ and $d^\dagger(d)$ for modes a, b, c and d . Using Eq.(3), one obtains the following transformations:

$$\begin{aligned} B_1 a^\dagger B_1^\dagger &= a^\dagger t_1 - c^\dagger r_1, & B_1 c^\dagger B_1^\dagger &= a^\dagger r_1 + c^\dagger t_1, \\ B_2 b^\dagger B_2^\dagger &= b^\dagger t_2 - d^\dagger r_2, & B_2 d^\dagger B_2^\dagger &= b^\dagger r_2 + d^\dagger t_2. \end{aligned} \quad (4)$$

where $t_j = \cos\theta_j$ and $r_j = \sin\theta_j$ ($j = 1, 2$) are the transmissivity and reflectivity of the beam splitter BS_j , respectively. The normalization factor p_{cd} represents the success probability heralded by the detection of a single photon at the modes c and d .

Using above relation and some technique (see Appendix A), the LQC-TMSVS $|\psi_{LQC}\rangle_{ab}$ can be expressed explicitly as follow

$$|\psi_{LQC}\rangle_{ab} = (c_0 + c_1 a^\dagger b^\dagger + c_2 a^{\dagger 2} b^{\dagger 2}) S_2(\lambda) |0_a, 0_b\rangle \quad (5)$$

where I introduce a new squeezing parameter λ satisfy $\tanh \lambda = t_1 t_2 \tanh r$ and set

$$\begin{aligned} c_0 &= \frac{t_1 t_2 \cosh \lambda}{\sqrt{p_{cd}} \cosh r}, \\ c_1 &= \frac{(r_1^2 r_2^2 - r_1^2 t_2^2 - r_2^2 t_1^2) \tanh r \cosh \lambda}{\sqrt{p_{cd}} \cosh r}, \\ c_2 &= \frac{r_1^2 r_2^2 \tanh r \sinh \lambda}{\sqrt{p_{cd}} \cosh r}. \end{aligned}$$

From Eq.(5), I find that the LQC-TMSVS $|\psi_{LQC}\rangle_{ab}$ is actually a superposition state of $S_2(\lambda) |0_a, 0_b\rangle$,

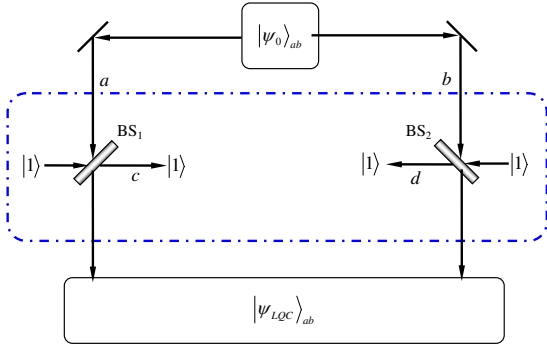


FIG. 2: (Colour online) Optical scheme to prepare a LQC-TMSVS by operating quantum-optical catalysis on each mode of a TMSVS. The input state is the TMSVS $|\psi_0\rangle_{ab}$ with the squeezing parameter r and the output state is the LQC-TMSVS $|\psi_{LQC}\rangle_{ab}$ related with the input and catalysis parameter. The catalysis parameters are determined by the transmissivity T_1 and T_2 of the tunable BS_1 and BS_2 , respectively. In contrast with the TMSVS, the LQC-TMSVS has a wide range of entanglement properties.

$a^\dagger b^\dagger S_2(\lambda) |0_a, 0_b\rangle$ and $a^{\dagger 2} b^{\dagger 2} S_2(\lambda) |0_a, 0_b\rangle$ with a certain ratio. Note that the coefficients c_0, c_1, c_2 and λ are all the functions of the input squeezing parameter r and the transmissivity t_1, t_2 of the BSs. Meanwhile, this state can also be looked as a non-Gaussian state by operating coherent superposition operator $(c_0 + c_1 a^\dagger b^\dagger + c_2 a^{\dagger 2} b^{\dagger 2})$ on $S_2(\lambda) |0_a, 0_b\rangle$. So I conclude that local quantum-optical catalysis operation plays the role of preparing the non-Gaussian entangled states. In the limit of $t_1 = t_2 = 1$, $|\psi_{LQC}\rangle_{ab} \rightarrow |\psi_0\rangle_{ab}$, i.e. the output state is just the input one. While at least one of t_1, t_2 is zero, leading to $\lambda = 0, c_0 = 0, c_1 = 1, c_2 = 0$, so $|\psi_{LQC}\rangle_{ab} \rightarrow |1_a, 1_b\rangle$, i.e. the output state is twin single-photon Fock state.

By the way, I often use the catalysis parameters $T_j = t_j^2$ ($j = 1, 2$) (i.e. the transmittance for each BS) in my following discussion and analysis. Compared with the input TMSVS, what optimal properties will emerge for the LQC-TMSVS? By tuning the input and catalysis parameters of the interaction, the LQC-TMSVS may be modulated, generating a wide range of entanglement phenomena, as I show next sections.

B. Success probability of detection

Normalization is important for discussing the properties of a quantum state. The normalization factor of the LQC-TMSVS is actually the probability p_{cd} of detecting successfully single photon at the modes c and d . The density operator of the LQC-TMSVS $\rho_{LQC} = |\psi_{LQC}\rangle_{ab} \langle\psi_{LQC}|$ is expressed in Appendix B. According to $\text{Tr}(\rho_{LQC}) = 1$, the success probability to get

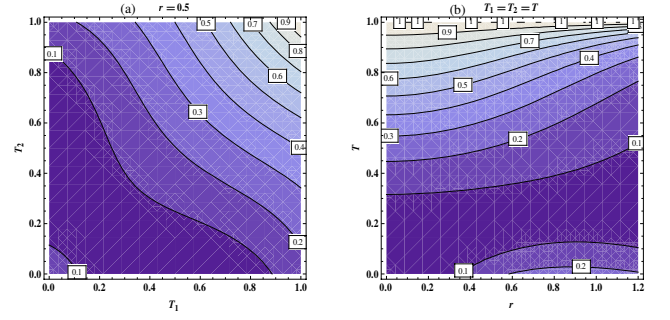


FIG. 3: (Color online) Success probability p_{cd} of detection as a function of the input parameter r and the catalysis parameter T_1, T_2 . (a) in (T_1, T_2) space for $r = 0.5$; (b) in (r, T) space.

$|\psi_{LQC}\rangle_{ab}$ from my proposal is given by

$$p_{cd} = p_0(a_0 + a_1 \tanh^2 r + a_2 \tanh^4 r + a_3 \tanh^6 r + a_4 \tanh^8 r), \quad (6)$$

with $p_0 = \cosh^{10} \lambda / \cosh^2 r$ and

$$\begin{aligned} a_0 &= t_1^2 t_2^2, \\ a_1 &= 1 - 4t_1^2 + 4t_1^4 - 4t_2^2 + 4t_2^4 + 16t_1^2 t_2^2 \\ &\quad - 16t_1^4 t_2^2 - 16t_1^2 t_2^4 + 11t_1^4 t_2^4, \\ a_2 &= 11t_1^2 t_2^2 - 28t_1^4 t_2^2 - 28t_1^2 t_2^4 + 64t_1^4 t_2^4 + 16t_1^6 t_2^2 \\ &\quad + 16t_1^2 t_2^6 - 28t_1^4 t_2^6 - 28t_1^6 t_2^4 + 11t_1^6 t_2^6, \\ a_3 &= 11t_1^4 t_2^4 - 16t_1^6 t_2^4 - 16t_1^4 t_2^6 + 4t_1^8 t_2^4 + 4t_1^4 t_2^8 \\ &\quad + 16t_1^6 t_2^6 - 4t_1^8 t_2^6 - 4t_1^6 t_2^8 + t_1^8 t_2^8, \\ a_4 &= t_1^6 t_2^6. \end{aligned}$$

In fig.3, I plot the distribution of the success probability p_{cd} in (T_1, T_2) space for $r = 0.5$ and in (r, T) space for the symmetric catalysis $T_1 = T_2 = T$. The maximin success probability is 1 for the limit case of $T_1 = T_2 = 1$. While at least one of T_1, T_2 is zero, $p_{cd} \rightarrow (1 - 2T_j)^2 \tanh^2 r / \cosh^2 r$ ($j = 1, 2$).

III. ENTANGLEMENT PROPERTIES

In contrast with the input TMSVS, can the local quantum-optical catalysis be useful to enhance the entanglement properties? If possible, then how can I adjust the catalysis parameters in the process of preparing the LQC-TMSVS? In this section, I shall discuss the entanglement properties of the LQC-TMSVS quantified by the von Neumann entropy and the EPR correlation.

A. Degree of entanglement

Entanglement for a pure state in Schmidt form, $|\psi\rangle_{ab} = \sum_n \omega_n |\alpha_n\rangle_a |\beta_n\rangle_b$ (ω_n real positive) with the orthonormal states $|\alpha_n\rangle_a$ and $|\beta_n\rangle_b$, is quantified by the

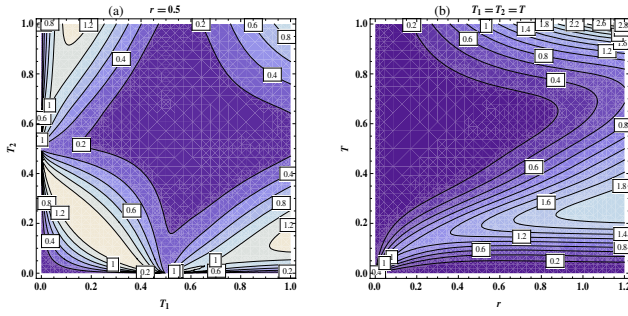


FIG. 4: (Color online) Neumann entropy E as a function of the input parameter r and the catalysis parameter T_1, T_2 . (a) in (T_1, T_2) space for $r = 0.5$; (b) in (r, T) space.

partial von Neumann entropy of the reduced density operator

$$E(|\psi\rangle_{ab}) = -\text{Tr}(\rho_a \log_2 \rho_a) = -\sum_n \omega_n^2 \log_2 \omega_n^2, \quad (7)$$

where the local state is given by $\rho_a = \text{Tr}_b(|\psi\rangle_{ab}\langle\psi|)$ [31]. The LQC-TMSVS $|\psi_{LQC}\rangle_{ab}$ written in Schmidt form yields

$$|\psi_{LQC}\rangle_{ab} = \sum_{n=0}^{\infty} \omega_n |n_a, n_b\rangle, \quad (8)$$

where the Schmidt coefficient is given by

$$\omega_n = \frac{(t_1^2 - n + nt_1^2)(t_2^2 - n + nt_2^2)(t_1 t_2)^{n-1} \tanh^n r}{\sqrt{p_{cd}} \cosh r}. \quad (9)$$

The entanglement amount of the LQC-TMSVS $E(|\psi_{LQC}\rangle_{ab})$ can be evaluated numerically by these Schmidt coefficients, as shown in Fig. 4.

In the limit cases, when at least one of t_1, t_2 is zero, the output state corresponding to $|1_a, 1_b\rangle$ is separate, $E = 0$. While $t_1 = t_2 = 1$, leading to $\omega_n^2 = \tanh^{2n} r / \cosh^2 r$, the output state is just the TMSVS (the input state), whose amount of entanglement is analytically given by [32, 33]

$$E(|\psi_0\rangle_{ab}) = \cosh^2 r \log_2 \cosh^2 r - \sinh^2 r \log_2 \sinh^2 r. \quad (10)$$

In order to understand whether the entanglement is enhanced by local quantum-optical catalysis, I compare the von Neumann entropy values between the LQC-TMSVSs and the TMSVSs. If $E(|\psi_{LQC}\rangle_{ab}) > E(|\psi_0\rangle_{ab})$, then the entanglement is enhanced in principle, else it is weakened.

There are three feasibility regions having $E(|\psi_{LQC}\rangle_{ab}) > E(|\psi_0\rangle_{ab})$, as shown in Fig. 5. One region is located in the small-catalysis parameter space, i.e. $T_1, T_2 \in (0, 0.5)$, the other two ones

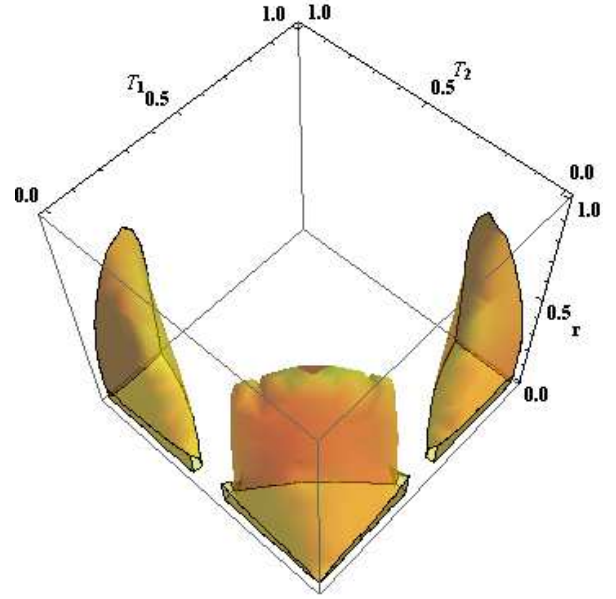


FIG. 5: (Color online) Three dimensional plot of the feasibility region for $E(|\psi_{LQC}\rangle_{ab}) > E(|\psi_0\rangle_{ab})$ in (r, T_1, T_2) space. But the true entanglement enhancement is only one of the three regions having small-squeezing and small-catalysis.

are located in one-small-one-large-catalysis parameter space, i.e. $T_1 \in (0, 0.5)$ but $T_2 \in (0.5, 1)$ or $T_2 \in (0, 0.5)$ but $T_1 \in (0.5, 1)$. Three sections of Fig. 5 with $r = 0.02, 0.2, 0.7$ is reshaped in Fig. 6. With increasing the input parameter r , the enhancement region decreases and disappears at threshold $r = 0.785$, as shown in Fig. 6. However, among the three regions in each figure, the true enhancing feasibility only happens in the small-squeezing ($0 < r < 0.785$) and small-catalysis ($T_1, T_2 \in (0, 0.5)$) regime. For example, when $r = 0.2$, $T_1 = 0.1$, $T_2 = 0.15$, $E(|\psi_0\rangle_{ab}) = 0.247116$, $E(|\psi_{LQC}\rangle_{ab}) = 1.03826$, the enhancement is true. However, the other two regions (one-small-one-large-catalysis) are actually the pseudo enhancement, because of the indeterminacy of $E(|\psi_{LQC}\rangle_{ab})$. For example, when $r = 0.2$, $T_1 = 0.1$, $T_2 = 0.8$, $E(|\psi_0\rangle_{ab}) = 0.247116$, but $E(|\psi_{LQC}\rangle_{ab})$ is indeterminate in my numerical calculation, so the enhancement is pseudo or can't judge.

Next I discuss the symmetric catalysis case, i.e. assuming $T = T_1 = T_2$. The feasibility region for enhancing the entanglement is depicted in the (r, T) plain space in Fig. 7. The enhancement happens in small-squeezing ($0 < r < 0.785$) and small-catalysis ($0 < T < 0.25$) regime. In Figs. 8. (a) I plot the von Neumann entropy $E(|\psi_{LQC}\rangle_{ab})$ as a function of the input squeezing parameter r for different $T = 0.1, 0.3$, compared with $T = 1$

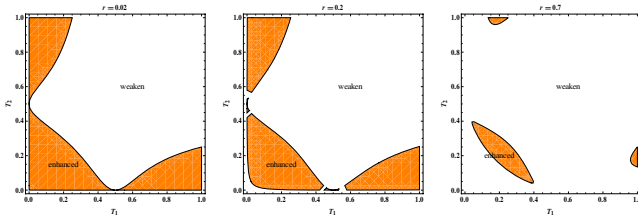


FIG. 6: (Color online) Plot of the feasibility region for $E(|\psi_{LQC}\rangle_{ab}) > E(|\psi_0\rangle_{ab})$ in (T_1, T_2) space with different $r = 0.02, 0.2, 0.7$, also three sections of Fig.5. But the true entanglement enhancement happen with small-squeezing and small-catalysis. If r is larger than a threshold value 0.785, the enhancement is impossible.

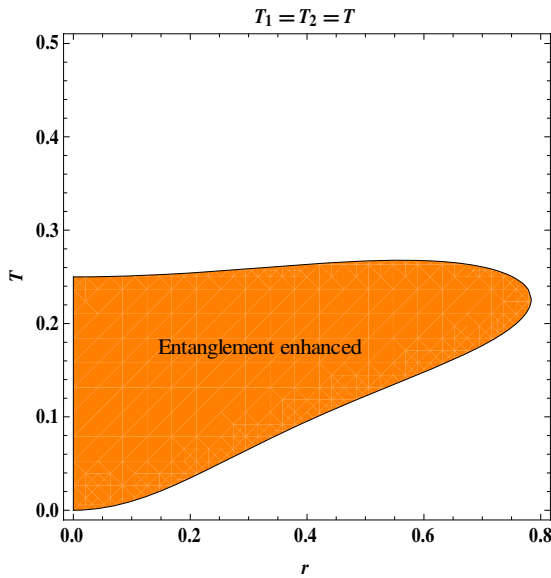


FIG. 7: (Color online) Plot of the feasibility region for enhancing entanglement, that is $E(|\psi_{LQC}\rangle_{ab}) > E(|\psi_0\rangle_{ab})$ in (r, T) space.

(corresponding to the input TMSVS). With reference to the curve of the TMSVS, one see that the enhancement is possible for $T = 0.1$ but not for $T = 0.3$. In Figs. 8. (b)-(d) I plot the von Neumann entropy $E(|\psi_{LQC}\rangle_{ab})$ as a function of the catalysis parameter T for different input parameter $r = 0.2, 0.785, 0.9$, each compared with their corresponding TMSVSs (the red dashed line). Obviously, for $r = 0.2$, the enhancement of entanglement will be happened in a certain catalysis range (about $(0.03, 0.23)$) (see Fig.8 (b)). But above threshold value $r = 0.785$, the enhancement is impossible, as shown in Fig.8 (d) for $r = 0.9$.

From above discussion, we conclude that the degree of entanglement measured by the von Neumann entropy turns out to be enhanced only in the small-squeezing and small-catalysis parameter space.

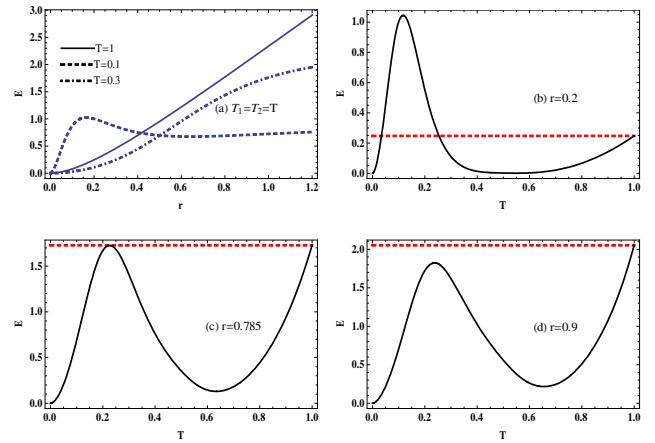


FIG. 8: (Color online) Neumann entropy $E(|\psi_{LQC}\rangle_{ab})$ are depicted in (a) as a function of the input squeezing parameter r for different $T = 0.1, 0.3$, compared with $T = 1$ (corresponding to the input TMSVS); in (b)-(d) as a function of the catalysis parameter T (black solid line) for (b) $r = 0.2$, (c) $r = 0.785$, (d) $r = 0.9$, respectively, compared with their TMSVSs (red dashed line).

B. Second-order Einstein-Podolsky-Rosen correlation

For two-mode Gaussian entangled states, entanglement can be fully described by the second-order Einstein-Podolsky-Rosen (EPR) correlation, which is characterized up to second-order moments of the state[34–36]. While for two-mode non-Gaussian entangled states, however, entanglement is fully described with all orders of moments[37, 38]. It is known to all that a TMSVS (Gaussian) is the correlated state of two field modes a and b (signal and idle) that can be generated by a nonlinear medium[39]. But after operating local quantum-optical catalysis on the TMSVS, how is the EPR correlation change? Here I further investigate the EPR correlation, another entanglement properties for the LQC-TMSVS.

The EPR correlation of two-mode states is the total variance of a pair of EPR-like operators,

$$\begin{aligned} \text{EPR} &= \Delta^2(x_a - x_b) + \Delta^2(p_a - p_b) \\ &= 2(1 + \langle a^\dagger a \rangle + \langle b^\dagger b \rangle - \langle a^\dagger b^\dagger \rangle - \langle ab \rangle) \\ &\quad - 2(\langle a \rangle - \langle b^\dagger \rangle)(\langle a^\dagger \rangle - \langle b \rangle), \end{aligned} \quad (11)$$

where $x_j = \frac{1}{\sqrt{2}}(j + j^\dagger)$ and $p_j = \frac{-i}{\sqrt{2}}(j - j^\dagger)$ ($j = a, b$). For separable two-mode states or any classical two-mode states, the total variance is larger than or equal to 2[34]. The condition $\text{EPR} < 2$, indicates quantum entanglement, which can be an important resource in continuous variable quantum information processing protocols.

Given a LQC-TMSVS, one can evaluate the EPR correlation with the expectation values in Eq.(11) according to the general expression of $\langle a^{\dagger k_1} b^{\dagger k_2} a^{l_1} b^{l_2} \rangle$ (see Appendix D) with corresponding (k_1, k_2, l_1, l_2) . Thus I

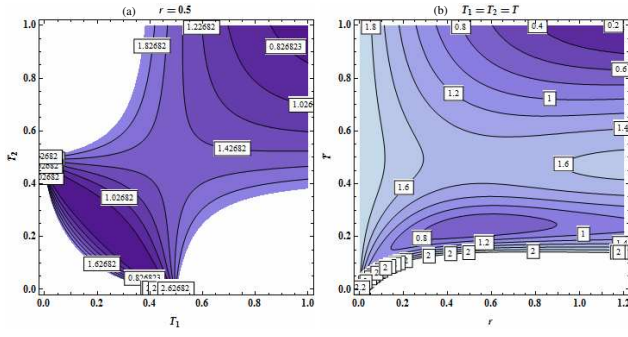


FIG. 9: (Color online) EPR correlation as a function of the input squeezing parameter r and the catalysis parameter T_1, T_2 . (a) in (T_1, T_2) space for $r = 0.5$; (b) in (r, T) space. The Colored region represents the condition $\text{EPR} < 2$.

prove that $\langle a^\dagger \rangle = \langle b^\dagger \rangle = \langle a \rangle = \langle b \rangle = 0$ and

$$\begin{aligned} \langle a^\dagger a \rangle = & M(x_0 + x_1 \tanh r + x_2 \tanh^2 r + x_3 \tanh^3 r \\ & + x_4 \tanh^4 r + x_5 \tanh^5 r + x_6 \tanh^6 r \\ & + x_7 \tanh^7 r + x_8 \tanh^8 r + x_9 \tanh^9 r), \quad (12) \end{aligned}$$

$$\begin{aligned} \langle b^\dagger b \rangle = & M(y_0 + y_1 \tanh r + y_2 \tanh^2 r + y_3 \tanh^3 r \\ & + y_4 \tanh^4 r + y_5 \tanh^5 r + y_6 \tanh^6 r \\ & + y_7 \tanh^7 r + y_8 \tanh^8 r + y_9 \tanh^9 r), \quad (13) \end{aligned}$$

as well as

$$\begin{aligned} \langle a^\dagger b^\dagger \rangle = \langle ab \rangle = & N(z_0 + z_1 \tanh r + z_2 \tanh^2 r \\ & + z_3 \tanh^3 r + z_4 \tanh^4 r + z_5 \tanh^5 r \\ & + z_6 \tanh^6 r + z_7 \tanh^7 r + z_8 \tanh^8 r), \quad (14) \end{aligned}$$

where I have set x_i s, y_i s, z_i s in Appendix E and

$$\begin{aligned} M &= (\cosh^{12} \lambda \tanh r) / (p_{cd} \cosh^2 r), \\ N &= (\cosh^{12} \lambda \tanh \lambda) / (p_{cd} \cosh^2 r). \end{aligned}$$

Upon substituting above equations into Eq.(11), the EPR correlation of the LQC-TMSVS $\text{EPR}(|\psi_{LQC}\rangle_{ab})$ can be calculated explicitly, which depends the input squeezing degree r and the catalysis parameters T_1, T_2 . In the limit of $T_1 = T_2 = 1$, $\text{EPR}(|\psi_{LQC}\rangle_{ab})$ reduces to $\text{EPR}(|\psi_0\rangle_{ab}) = 2e^{-2r}$, which tends to zero asymptotically for $r \rightarrow \infty$. In Fig.9, we plot the EPR correlation of the LQC-TMSVS in (T_1, T_2) space for $r = 0.5$ and in (r, T) space under the condition $\text{EPR} < 2$. One can see that there exists a threshold curve (boundary of $\text{EPR} = 2$) as a function of T_1 and T_2 for $r = 0.5$ in Fig.9(a) and as a function of λ and T in Fig.9(b), respectively.

To exhibit whether the EPR correlation is enhanced, the fact that $\text{EPR}(|\psi_{LQC}\rangle_{ab})$ must be smaller than $\text{EPR}(|\psi_0\rangle_{ab})$ must be hold. The feasibility enhancement region of the EPR correlation is shown in Fig.10. Three

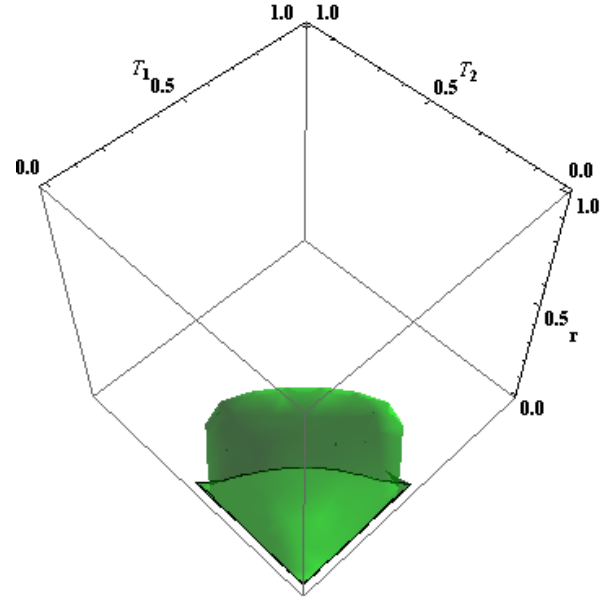


FIG. 10: (Colour online) Three dimensional plot of the feasibility region for enhancing EPR correlation, that is $\text{EPR}(|\psi_{LQC}\rangle_{ab}) < \text{EPR}(|\psi_0\rangle_{ab})$, in (r, T_1, T_2) space.

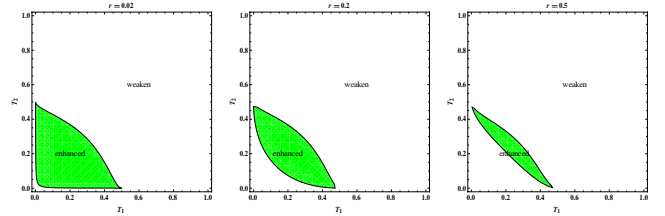


FIG. 11: (Color online) Plot of the feasibility region for enhancing EPR correlation, that is $\text{EPR}(|\psi_{LQC}\rangle_{ab}) < \text{EPR}(|\psi_0\rangle_{ab})$, in (T_1, T_2) space with different $r = 0.02, 0.2, 0.5$, also three sections of Fig.10. If r is larger than a threshold value 0.585 , the enhancement is impossible.

sections of Fig.10 are shown in Fig.11. Obviously, the enhancement is happened only in one region with small-squeezing and small-catalysis, unlike that of the degree of entanglement in Fig.5 and Fig.6. Moreover, with increasing the input parameter r , the enhancement region decrease and disappear at threshold $r = 0.585$.

The feasibility region for enhancing the EPR correlation is depicted in the (r, T) plain space in Fig.12. For a small-squeezing ($0 < r < 0.585$) and small-catalysis ($0 < T < 0.3$), the quantum-optical catalysis enhance the EPR correlation of the TMSVS (see Fig.2). In Fig.13 I plot the EPR correlation of the LQC-TMSVS as a function of r or T . In general, the EPR correlation of the TMSVS is enhanced with the squeezing parameter r , but it may not be always true for the case of $T = 0.1$, as shown in Fig.13 (a). I particularly compare the EPR correlation

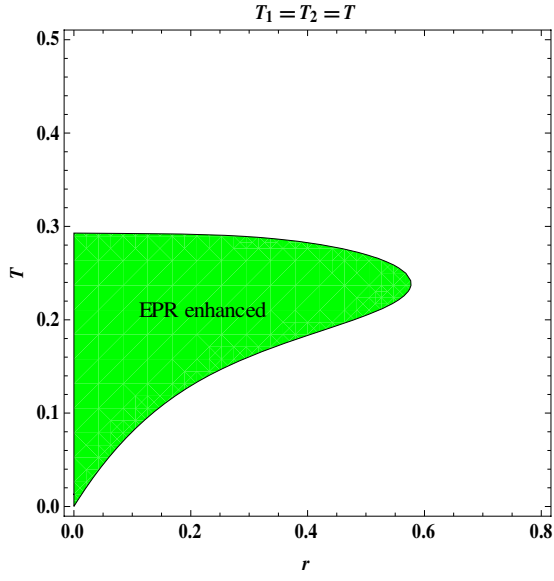


FIG. 12: (Color online) Plot of the feasibility region for enhancing EPR correlation, that is $\text{EPR}(|\psi_{LQC}\rangle_{ab}) < \text{EPR}(|\psi_0\rangle_{ab})$ in (r, T) space.

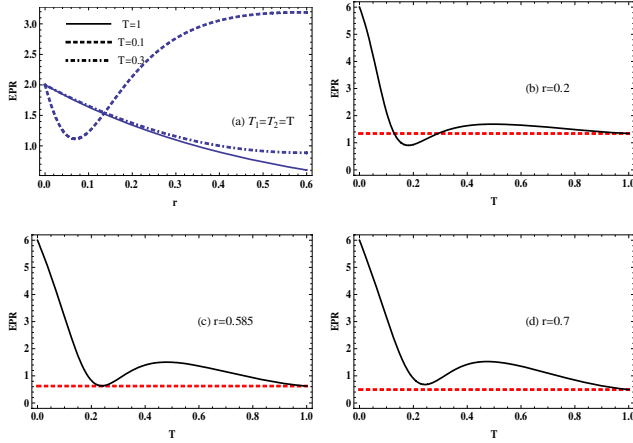


FIG. 13: (Colour online) (a) EPR correlation as a function of the input parameter r for different $T = 0.1, 0.3$, compared with $T = 1$ (corresponding to the input TMSVS); in (b)-(d) as a function of T for different input parameter $r = 0.2, 0.585, 0.7$, compared with their TMSVSs (the red dashed line).

of the LQC-TMSVS with that of the TMSVS for the cases $r = 0.2, 0.585, 0.7$ in Fig.13 (b)-(d). For a modern catalysis parameter $0.12 < T < 0.3$, the catalysis operation gives the better EPR correlation for $r = 0.2$, where a rather large squeezing $r > 0.585$, the quantum-optical catalysis becomes the worse operation.

IV. QUANTUM TELEPORTATION USING NON-GAUSSIAN ENTANGLED STATE

After employing local quantum-optical catalysis on the TMSVS, I can see that the degree of entanglement and the EPR correlation can be enhanced in small-squeezing and small-catalysis parameter regime. Now I consider the LQC-TMSVS as entangled resources in the Braunstein and Kimble (BK) protocol[1] to teleport a coherent state $|\gamma\rangle$ in CV teleportation. The fidelity between an input state and the output state is usually used as a measure to describe the quality of the quantum teleportation (QT).

For a CV system, a teleportation scheme has been proposed according to the characteristic functions (CFs) of the quantum states concluding input, source and teleported states[40]. For the input coherent state, it is sufficient to calculate the teleportation fidelity for a particular input coherent state since there is no difference between the amplitudes of the input and output coherent states in the BK protocol. For brevity I take $\gamma = 0$, and then I only calculate the fidelity of teleporting the input vacuum state with the CF $\chi_{in}(z) = \exp[-|z|^2/2]$. The CF of the LQC-TMSVS (entangled resource or channel) $|\psi_{LQC}\rangle_{ab}$ is given by

$$\chi_E(\alpha, \beta) = \text{Tr}(D_a(\alpha) D_b(\beta) \rho_{LQC}), \quad (15)$$

where $D_a(\alpha) = e^{\alpha a^\dagger - \alpha^* a}$, $D_b(\beta) = e^{\beta b^\dagger - \beta^* b}$ are the displacement operators. The detailed calculation procedure and result of $\chi_E(\alpha, \beta)$ are shown in Appendix F. The CF $\chi_{out}(z)$ of the output state can be related to the CFs of the input state and the entangled source by formula $\chi_{out}(z) = \chi_{in}(z) \chi_E(z^*, z)$. Hence the fidelity of QT of CVs can be obtained as[41]

$$F = \int \frac{d^2 z}{\pi} \chi_{in}(-z) \chi_{out}(z). \quad (16)$$

Thus F yields

$$F = \frac{p_0}{4p_{cd}} (m_0 + m_1 \tanh r + m_2 \tanh^2 r + m_3 \tanh^3 r + m_4 \tanh^4 r), \quad (17)$$

where

$$\begin{aligned} m_0 &= 2t_1^2 t_2^2, \\ m_1 &= 2t_1 t_2 - 4t_1^3 t_2 - 4t_1 t_2^3 - 2t_1^3 t_2^3, \\ m_2 &= 1 - 4t_1^2 + 4t_1^4 - 4t_2^2 + 4t_2^4 + 10t_1^2 t_2^2 \\ &\quad - 2t_1^4 t_2^2 - 2t_1^2 t_2^4 + 5t_1^4 t_2^4, \\ m_3 &= t_1 t_2 - t_1^3 t_2 - 2t_1^5 t_2 - t_1 t_2^3 - 2t_1 t_2^5 \\ &\quad - 2t_1^3 t_2^3 + t_1^5 t_2^3 + t_1^3 t_2^5 - 3t_1^5 t_2^5, \\ m_4 &= t_1^2 t_2^2 - t_1^4 t_2^2 + t_1^6 t_2^2 - t_1^2 t_2^4 + t_1^2 t_2^6 \\ &\quad + 2t_1^4 t_2^4 - t_1^6 t_2^4 - t_1^4 t_2^6 + t_1^6 t_2^6. \end{aligned}$$

In the limit case of $t_1^2 = t_2^2 = 1$, the fidelity of LQC-TMSVS $F(|\psi_{LQC}\rangle_{ab})$ reduces to that of the TMSVS

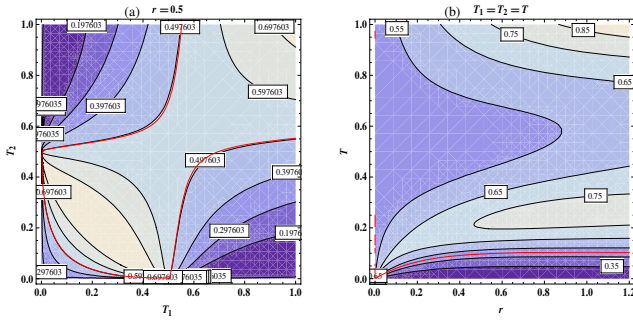


FIG. 14: (Color online) Teleportation fidelity of a coherent state with the LQC-TMSVS as a function of the input squeezing parameter r and the catalysis parameter T_1, T_2 . (a) in (T_1, T_2) space for $r = 0.5$; (b) in (r, T) space. The red line is the boundary with $F = 0.5$.

$F(|\psi_0\rangle_{ab}) = (1 + \tanh r)/2$, which is 0.5 for $r = 0$ and tends to 1 asymptotically for $r \rightarrow \infty$. In Fig.14, we show the fidelity of teleportating a coherent state using the resource (LQC-TMSVS) in (T_1, T_2) space for $r = 0.5$ and in (r, T) space. The red line denotes the boundary with $F = 0.5$. The fidelity over the classical limit 0.5 may be considered as a successful quantum protocol[42].

Similar analysis of the teleportation fidelity are performed like that of the degree of entanglement and the EPR correlation in Sec. III. In Fig.15, I plot the feasibility region for enhancing teleportation fidelity of a coherent state with the LQC-TMSVS, that is $F(|\psi_{LQC}\rangle_{ab}) > F(|\psi_0\rangle_{ab})$, in (r, T_1, T_2) space. Figures of Fig.16 are three sections of Fig.15 with $r = 0.02, 0.2, 0.5$. In Fig.17, I display the feasibility region in (r, T) space for enhancing teleportation fidelity of a coherent state using the LQC-TMSVS. The teleportation fidelity as a function of r or T are plotted in Fig.18. Compared with the TMSVS as the entangled resource, the enhancement of the teleportation fidelity is found in the range of $0 < r < 0.6$ and $0 < T < 0.27$. All these figures indicate that local quantum-optical catalysis can enhance the teleportation fidelity at the small-squeezing and small-catalysis parameter regime.

V. DISCUSSION AND CONCLUSION

Interesting, by comparing the figures of the degree of entanglement (orange), the EPR correlation (green) and the teleportation fidelity (red) of the LQC-TMSVS in Figs.5,10,15 and Figs.7,12,17, I see that these enhancement regions do not overlap completely and locate in different input and catalysis parameter intervals. Taking the symmetric catalysis as example, the enhancement regions are different as (i) $0 < r < 0.785$ and $0 < T < 0.25$ for the degree of entanglement (ii) $0 < r < 0.585$ and $0 < T < 0.3$ for the EPR correlation; (iii) $0 < r < 0.6$ and $0 < T < 0.27$ for the teleportation fidelity. I fur-

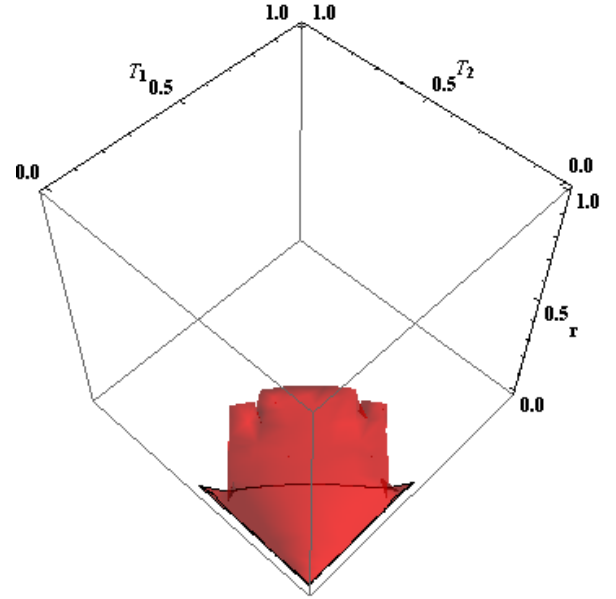


FIG. 15: (Color online) Three dimensional plot of the feasibility region for enhancing teleportation fidelity of a coherent state with the LQC-TMSVS, that is $F(|\psi_{LQC}\rangle_{ab}) > F(|\psi_0\rangle_{ab})$, in (r, T_1, T_2) space.

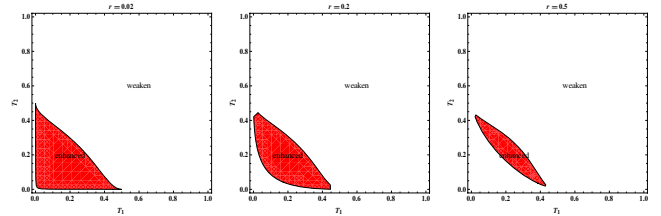


FIG. 16: (Color online) Plot of the feasibility region for enhancing teleportation fidelity of a coherent state with the LQC-TMSVS, that is $F(|\psi_{LQC}\rangle_{ab}) > F(|\psi_0\rangle_{ab})$ in (T_1, T_2) space with different $r = 0.02, 0.2, 0.5$, also three sections of Fig.15. If r is larger than a threshold value 0.6, the enhancement is impossible.

ther reshape each two of the three plots (Figs.7,12,17) in the same graph, as shown in Fig.19. The conclusions are concluded by answering the question of 'If A is enhanced, then B must be enhanced?', as demonstrated in Table I. For instance, there exists a parameter region where no EPR correlation enhancement, nevertheless, the fidelity enhancement is achieved (see the red area in Fig.19 (f)), so my answer is 'no'. Meanwhile it is found that all the enhancements have the common regions, i.e. the small-squeezing ($0 < r < 0.585$) and small-catalysis ($0 < T < 0.25$ or $0 < T_1, T_2 < 0.5$) regime, as shown in Fig.20. All these results may thus carry a practical significance.

In summary, I have proposed an optical scheme to

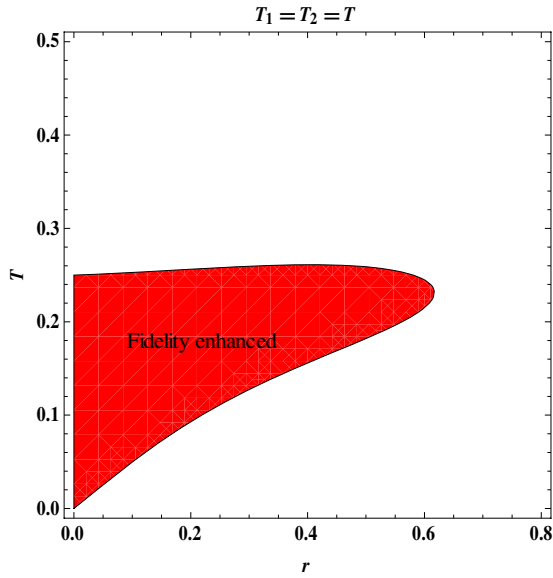


FIG. 17: (Color online) Plot of the feasibility region for enhancing teleportation fidelity of a coherent state with the LQC-TMSVS, that is $F(|\psi_{LQC}\rangle_{ab}) > F(|\psi_0\rangle_{ab})$ in (r, T) space.

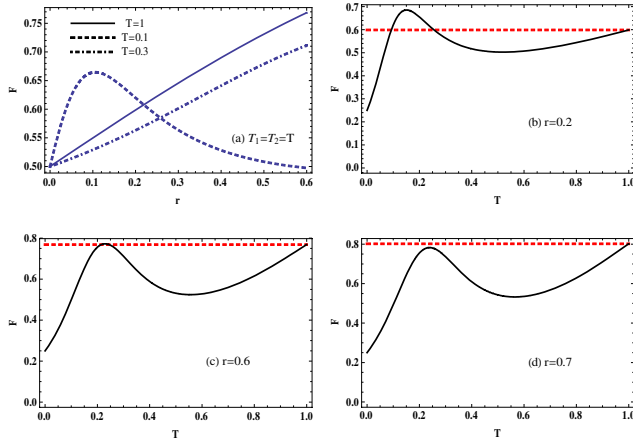


FIG. 18: (Color online) (a) Teleportation fidelity of a coherent state with the LQC-TMSVS as a function of the input parameter r for different $T = 0.1, 0.3$, compared with $T = 1$ (corresponding to the input TMSVS); in (b)-(d) as a function of T for different input parameter $r = 0.2, 0.6, 0.7$, compared with their TMSVSs (the red dashed line).

TABLE I: If A is enhanced, then B must be enhanced?

case	A	B	answer
Fig.19(a)	E	EPR	no
Fig.19(b)	EPR	E	no
Fig.19(c)	E	F	no
Fig.19(d)	F	E	yes
Fig.19(e)	EPR	F	no
Fig.19(f)	F	EPR	no

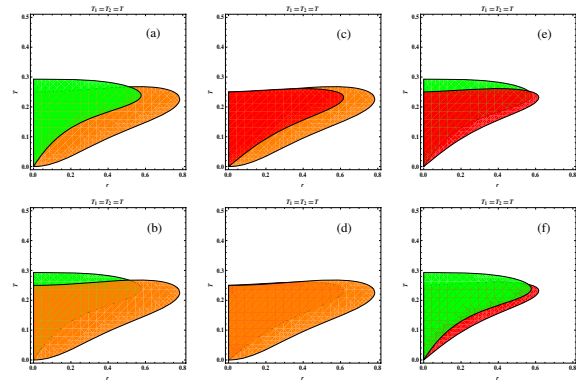


FIG. 19: (Colour online) Comparison of the enhancing feasibility region for each two of the three properties, i.e. the degree of entanglement (orange, E), EPR correlation (green, EPR) and teleportation fidelity (red, F) in (r, T) space for symmetric catalysis. (a) E under EPR; (b) EPR under E; (c) E under F; (d) F under E; (e) EPR under F; (f) F under EPR. The stack-ups indicate the enhancement difference of these three properties. The illustration is explained in Table I.

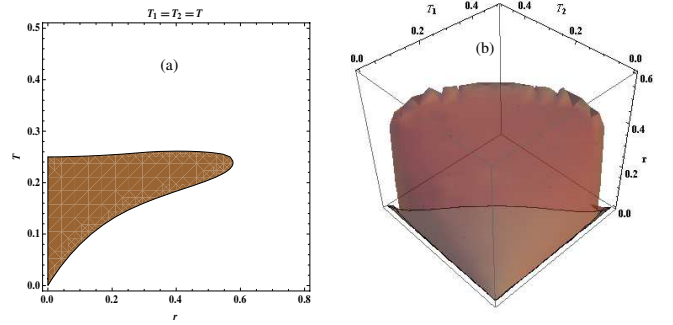


FIG. 20: (Colour online) The common feasibility region for enhancing entanglement, EPR correlation and teleportation fidelity in (r, T) space (a) and in (r, T_1, T_2) space (b). The brown region are located at small-squeezing and small-catalysis regime.

preparing a non-Gaussian two-mode quantum state, i.e. the LQC-TMSVS. In fact, for a fair comparison between the LQC-TMSVS and the TMSVS, I have shown that the local quantum-optical catalysis can enhance the entanglement properties including the degree of entanglement, the EPR correlation, and the quantum teleportation fidelity by adjusting appropriate catalysis parameter. The present study can be further pursued to include other two-mode input states than the TMSVS and quantum-optical catalysis on each mode. In view of the quantum-optical catalysis, my proposal can provide a potential and practical advantage for various quantum information tasks, such as quantum metrology and quantum computation.

Appendix A: the explicit form of $|\psi_{LQC}\rangle_{ab}$

In this appendix, I derive the the explicit form of

$|\psi_{LQC}\rangle_{ab}$. Noting the integral form of $|\psi_{LQC}\rangle_{ab}$,

$$|\Psi\rangle_{ab} = \frac{1}{\sinh r} \int \frac{d^2\alpha}{\pi} e^{-|\alpha|^2 \tanh^{-1} r + \alpha a^\dagger + \alpha^* b^\dagger} |0, 0\rangle$$

and the differential form of Fock state $|1\rangle$, such as $|1_c\rangle = \frac{d}{ds_1} e^{s_1 c^\dagger} |0_c\rangle$ and $|1_d\rangle = \frac{d}{ds_2} e^{s_2 d^\dagger} |0_d\rangle$, I rewrite $|\psi_{LQC}\rangle_{ab}$ as

$$\begin{aligned} & |\psi_{LQC}\rangle_{ab} \\ &= \frac{1}{\sqrt{p_{cd}} \sinh r} \frac{d^4}{ds_1 ds_2 ds_3 ds_4} \int \frac{d^2\alpha}{\pi} e^{-|\alpha|^2 \tanh^{-1} r} \\ & \langle 0_c | e^{s_3 c} B_1 e^{\alpha a^\dagger} e^{s_1 c^\dagger} B_1^\dagger |0_a\rangle |0_c\rangle \\ & \langle 0_d | e^{s_4 d} B_2 e^{\alpha^* b^\dagger} e^{s_2 d^\dagger} B_2^\dagger |0_b\rangle |0_d\rangle |_{(s_1, s_2, s_3, s_4)=0}. \end{aligned}$$

where $(s_1, s_2, s_3, s_4) = 0$ denotes $s_1 = s_2 = s_3 = s_4 = 0$. Further using the transformation in Eq.(3), $B_1 |0_a\rangle |0_c\rangle = |0_a\rangle |0_c\rangle$ and $B_2 |0_b\rangle |0_d\rangle = |0_b\rangle |0_d\rangle$, I have

$$\begin{aligned} & |\psi_{LQC}\rangle_{ab} \\ &= \frac{1}{\sqrt{p_{cd}} \sinh r} \frac{d^4}{ds_1 ds_2 ds_3 ds_4} \int \frac{d^2\alpha}{\pi} e^{-|\alpha|^2 \tanh^{-1} r} \\ & \langle 0_c | e^{s_3 c} e^{c^\dagger (s_1 t_1 - \alpha r_1)} |0_c\rangle \langle 0_d | e^{s_4 d} e^{d^\dagger (s_2 t_2 - \alpha^* r_2)} |0_d\rangle \\ & e^{a^\dagger (\alpha t_1 + s_1 r_1)} |0_a\rangle \otimes e^{b^\dagger (s_2 r_2 + \alpha^* t_2)} |0_b\rangle |_{(s_1, s_2, s_3, s_4)=0}. \end{aligned}$$

Inserting the completeness relation of coherent state $\int \frac{d^2 z_j}{\pi} |z_j\rangle \langle z_j| = 1$ ($j = 1, 2$) in appropriate place, I have

$$\begin{aligned} & |\psi_{LQC}\rangle_{ab} \\ &= \frac{1}{\sqrt{p_{cd}} \sinh r} \frac{d^4}{ds_1 ds_2 ds_3 ds_4} \int \frac{d^2\alpha}{\pi} e^{-|\alpha|^2 \tanh^{-1} r} \\ & \langle 0_c | e^{s_3 c} \int \frac{d^2 z_1}{\pi} |z_1\rangle \langle z_1| e^{c^\dagger (s_1 t_1 - \alpha r_1)} |0_c\rangle \\ & \langle 0_d | e^{s_4 d} \int \frac{d^2 z_2}{\pi} |z_2\rangle \langle z_2| e^{d^\dagger (s_2 t_2 - \alpha^* r_2)} |0_d\rangle \\ & e^{a^\dagger (\alpha t_1 + s_1 r_1) + b^\dagger (s_2 r_2 + \alpha^* t_2)} |0_a, 0_b\rangle |_{(s_1, s_2, s_3, s_4)=0} \end{aligned}$$

After a straightforward integration, I finally arrive at the derivative form of $|\psi_{LQC}\rangle_{ab}$,

$$\begin{aligned} |\psi_{LQC}\rangle_{ab} &= \frac{1}{\sqrt{p_{cd}} \cosh r} \frac{d^4}{ds_1 ds_2 ds_3 ds_4} \\ & e^{+s_3 s_4 r_1 r_2 \tanh r + s_1 s_3 t_1 + s_2 s_4 t_2} \\ & e^{+a^\dagger s_1 r_1 - a^\dagger s_4 t_1 r_2 \tanh r + b^\dagger s_2 r_2 - b^\dagger s_3 t_2 r_1 \tanh r} \\ & e^{a^\dagger b^\dagger t_1 t_2 \tanh r} |0_a, 0_b\rangle |_{(s_1, s_2, s_3, s_4)=0}. \end{aligned}$$

Therefore the explicit form in Eq.(5) can be obtained after making derivation.

Appendix B: the density operator $\rho_{LQC} = |\psi_{LQC}\rangle_{ab} \langle \psi_{LQC}|$

The conjugate state of $|\psi_{LQC}\rangle_{ab}$ can be given by

$$\begin{aligned} & {}_{ab} \langle \psi_{LQC}| \\ &= \frac{1}{\sqrt{p_{cd}} \cosh r} \frac{d^4}{dh_1 dh_2 dh_3 dh_4} \langle 0_a, 0_b | e^{abt_1 t_2 \tanh r} \\ & e^{+ah_1 r_1 - ah_4 t_1 r_2 \tanh r + bh_2 r_2 - bh_3 t_2 r_1 \tanh r} \\ & e^{+h_3 h_4 r_1 r_2 \tanh r + h_1 h_3 t_1 + h_2 h_4 t_2} |_{(h_1, h_2, h_3, h_4)=0} \end{aligned}$$

Then the density operator is

$$\begin{aligned} & \rho_{LQC} \\ &= \frac{1}{p_{cd} \cosh^2 r} \frac{d^8}{ds_1 ds_2 ds_3 ds_4 dh_1 dh_2 dh_3 dh_4} \\ & e^{+s_3 s_4 r_1 r_2 \tanh r + s_1 s_3 t_1 + s_2 s_4 t_2} \\ & e^{+h_3 h_4 r_1 r_2 \tanh r + h_1 h_3 t_1 + h_2 h_4 t_2} \\ & e^{a^\dagger s_1 r_1 - a^\dagger s_4 t_1 r_2 \tanh r + b^\dagger s_2 r_2 - b^\dagger s_3 t_2 r_1 \tanh r} \\ & e^{a^\dagger b^\dagger t_1 t_2 \tanh r} |0_a, 0_b\rangle \langle 0_a, 0_b| e^{abt_1 t_2 \tanh r} \\ & e^{ah_1 r_1 - ah_4 t_1 r_2 \tanh r + bh_2 r_2 - bh_3 t_2 r_1 \tanh r} \\ & |_{(s_1, s_2, s_3, s_4, h_1, h_2, h_3, h_4)=0}. \end{aligned}$$

Appendix C: Success probability of detection

Due to $\text{Tr}(\rho_{LQC}) = 1$, I have

$$p_{cd} = \frac{\cosh^2 \lambda}{\cosh^2 r} \frac{d^8}{ds_1 ds_2 ds_3 ds_4 dh_1 dh_2 dh_3 dh_4} \exp(\Xi) |_{(s_1, s_2, s_3, s_4, h_1, h_2, h_3, h_4)=0},$$

where I have set

$$\begin{aligned} \Xi &= +\epsilon_1 (s_3 s_4 + h_3 h_4) + \epsilon_2 (s_1 s_2 + h_1 h_2) \\ & + \epsilon_3 (s_1 s_3 + h_1 h_3) + \epsilon_4 (s_2 s_4 + h_2 h_4) \\ & - \epsilon_5 (h_2 s_3 + s_2 h_3) - \epsilon_6 (s_4 h_1 + s_1 h_4) \\ & + \epsilon_7 s_1 h_1 + \epsilon_8 s_2 h_2 + \epsilon_9 s_3 h_3 + \epsilon_{10} s_4 h_4 \end{aligned}$$

with

$$\begin{aligned} \epsilon_1 &= \frac{r_1 r_2 \sinh 2\lambda}{2t_1 t_2}, \epsilon_2 = \frac{r_1 r_2 \sinh 2\lambda}{2}, \\ \epsilon_3 &= t_1 \cosh^2 \lambda - \frac{\sinh^2 \lambda}{t_1}, \\ \epsilon_4 &= t_2 \cosh^2 \lambda - \frac{\sinh^2 \lambda}{t_2} \\ \epsilon_5 &= \frac{r_1 r_2 \sinh 2\lambda}{2t_1}, \epsilon_6 = \frac{r_1 r_2 \sinh 2\lambda}{2t_2} \\ \epsilon_7 &= r_1^2 \cosh^2 \lambda, \epsilon_8 = r_2^2 \cosh^2 \lambda \\ \epsilon_9 &= \frac{r_1^2 \sinh^2 \lambda}{t_1^2}, \epsilon_{10} = \frac{r_2^2 \sinh^2 \lambda}{t_2^2}. \end{aligned}$$

Appendix D: Expectation value of $\langle a^{\dagger k_1} b^{\dagger k_2} a^{l_1} b^{l_2} \rangle$

According to $\langle a^{\dagger k_1} b^{\dagger k_2} a^{l_1} b^{l_2} \rangle = \text{Tr}(a^{\dagger k_1} b^{\dagger k_2} a^{l_1} b^{l_2} \rho_{LQC})$ and making detailed calcu-

lation, I obtain

$$\begin{aligned} & \langle a^{\dagger k_1} b^{\dagger k_2} a^{l_1} b^{l_2} \rangle \\ &= \frac{\cosh^2 \lambda}{p_{cd} \cosh^2 r} \frac{d^{8+k_1+l_1+k_2+l_2}}{ds_1 ds_2 ds_3 ds_4 dh_1 dh_2 dh_3 dh_4 df_1^{k_1} df_2^{l_1} dg_1^{k_2} dg_2^{l_2}} \\ & \exp(\Xi + \Theta) |_{(s_1, s_2, s_3, s_4, h_1, h_2, h_3, h_4, f_1, f_2, g_1, g_2)=0}, \end{aligned}$$

where I have set

$$\begin{aligned} \Theta = & +\eta_1 (s_1 g_1 + h_1 g_2) + \eta_2 (s_2 f_1 + h_2 f_2) \\ & +\eta_3 (s_2 g_2 + h_2 g_1) + \eta_4 (s_1 f_2 + h_1 f_1) \\ & -\eta_5 (s_3 g_2 + h_3 g_1) - \eta_6 (s_4 f_2 + h_4 f_1) \\ & -\eta_7 (s_4 g_1 + h_4 g_2) - \eta_8 (s_3 f_1 + h_3 f_2) \\ & +\eta_9 (f_1 g_1 + f_2 g_2) + \eta_{10} (f_1 f_2 + g_1 g_2) \end{aligned}$$

with

$$\begin{aligned} \eta_1 &= \frac{r_1 \sinh 2\lambda}{2}, \eta_2 = \frac{r_2 \sinh 2\lambda}{2}, \\ \eta_3 &= r_2 \cosh^2 \lambda, \eta_4 = r_1 \cosh^2 \lambda, \\ \eta_5 &= \frac{r_1 \sinh 2\lambda}{2t_1}, \eta_6 = \frac{r_2 \sinh 2\lambda}{2t_2}, \\ \eta_7 &= \frac{r_2 \sinh^2 \lambda}{t_2}, \eta_8 = \frac{r_1 \sinh^2 \lambda}{t_1}, \\ \eta_9 &= \frac{\sinh 2\lambda}{2}, \eta_{10} = \sinh^2 \lambda. \end{aligned}$$

Appendix E.: the expressions of x_i s, y_i s, z_i s

Here I list the expressions of x_i s, y_i s, z_i s as follow

$$\begin{aligned} x_0 &= -2t_1^2 t_2^4 + 2t_1^4 t_2^4, \\ x_1 &= 1 - 4t_1^2 + 4t_1^4 - 4t_2^2 + 4t_2^4 + 16t_1^2 t_2^2 - 16t_1^4 t_2^2 \\ & \quad - 14t_1^2 t_2^4 + 14t_1^4 t_2^4 + t_1^6 t_2^6 - 2t_1^4 t_2^6 + t_1^6 t_2^6, \\ x_2 &= 4t_1^2 t_2^2 - 12t_1^4 t_2^2 + 8t_1^6 t_2^2 - 16t_1^2 t_2^4 + 48t_1^4 t_2^4 \\ & \quad - 32t_1^6 t_2^4 + 14t_1^2 t_2^6 - 34t_1^4 t_2^6 + 20t_1^6 t_2^6, \\ x_3 &= 22t_1^2 t_2^2 - 60t_1^4 t_2^2 + 40t_1^6 t_2^2 - 56t_1^2 t_2^4 + 146t_1^4 t_2^4 \\ & \quad - 92t_1^6 t_2^4 + 2t_1^8 t_2^4 + 33t_1^2 t_2^6 - 92t_1^4 t_2^6 + 61t_1^6 t_2^6 \\ & \quad - 8t_1^8 t_2^6 + 4t_1^4 t_2^8 - 8t_1^6 t_2^8 + 4t_1^8 t_2^8, \\ x_4 &= 24t_1^4 t_2^4 - 52t_1^6 t_2^4 + 28t_1^8 t_2^4 - 48t_1^4 t_2^6 + 88t_1^6 t_2^6 \\ & \quad - 40t_1^8 t_2^6 + 20t_1^4 t_2^8 - 34t_1^6 t_2^8 + 14t_1^8 t_2^8, \\ x_5 &= 40t_1^4 t_2^4 - 76t_1^6 t_2^4 + 30t_1^8 t_2^4 - 76t_1^4 t_2^6 + 140t_1^6 t_2^6 \\ & \quad - 56t_1^8 t_2^6 + 4t_1^{10} t_2^6 + 36t_1^4 t_2^8 - 58t_1^6 t_2^8 + 26t_1^8 t_2^8 \\ & \quad - 4t_1^{10} t_2^8 + t_1^6 t_2^{10} - 2t_1^8 t_2^{10} + t_1^{10} t_2^{10}, \\ x_6 &= 8t_1^6 t_2^6 - 8t_1^8 t_2^6 - 8t_1^6 t_2^8 + 8t_1^8 t_2^8 + 2t_1^6 t_2^{10} - 2t_1^8 t_2^{10}, \\ x_7 &= 14t_1^6 t_2^6 - 16t_1^8 t_2^6 + 4t_1^{10} t_2^6 - 20t_1^6 t_2^8 + 16t_1^8 t_2^8 \\ & \quad - 4t_1^{10} t_2^8 + 5t_1^6 t_2^{10} - 4t_1^8 t_2^{10} + t_1^{10} t_2^{10}, \\ x_8 &= 0, \quad x_9 = t_1^8 t_2^8, \end{aligned}$$

$$\begin{aligned} y_0 &= -2t_1^4 t_2^2 + 2t_1^2 t_2^4, \\ y_1 &= 1 - 4t_1^2 + 4t_1^4 - 4t_2^2 + 4t_2^4 + 16t_1^2 t_2^2 - 16t_1^4 t_2^2 \\ & \quad - 14t_1^2 t_2^4 + 14t_1^4 t_2^4 + t_1^6 t_2^6 - 2t_1^4 t_2^6 + t_1^6 t_2^6, \\ y_2 &= 4t_1^2 t_2^2 - 16t_1^4 t_2^2 + 14t_1^6 t_2^2 - 12t_1^2 t_2^4 + 48t_1^4 t_2^4 \\ & \quad - 34t_1^6 t_2^4 + 8t_1^2 t_2^6 - 32t_1^4 t_2^6 + 20t_1^6 t_2^6, \\ y_3 &= 22t_1^2 t_2^2 - 56t_1^4 t_2^2 + 33t_1^6 t_2^2 - 60t_1^2 t_2^4 + 146t_1^4 t_2^4 \\ & \quad - 92t_1^6 t_2^4 + 4t_1^8 t_2^4 + 40t_1^2 t_2^6 - 92t_1^4 t_2^6 + 61t_1^6 t_2^6 \\ & \quad - 8t_1^8 t_2^6 + 2t_1^4 t_2^8 - 8t_1^6 t_2^8 + 4t_1^8 t_2^8, \\ y_4 &= 24t_1^4 t_2^4 - 48t_1^6 t_2^4 + 20t_1^8 t_2^4 - 52t_1^4 t_2^6 + 88t_1^6 t_2^6 \\ & \quad - 34t_1^8 t_2^6 + 28t_1^4 t_2^8 - 40t_1^6 t_2^8 + 14t_1^8 t_2^8, \\ y_5 &= 40t_1^4 t_2^4 - 76t_1^6 t_2^4 + 36t_1^8 t_2^4 - 76t_1^4 t_2^6 + 140t_1^6 t_2^6 \\ & \quad - 58t_1^8 t_2^6 + t_1^{10} t_2^6 + 30t_1^4 t_2^8 - 56t_1^6 t_2^8 + 26t_1^8 t_2^8 \\ & \quad - 2t_1^{10} t_2^8 + 4t_1^6 t_2^{10} - 4t_1^8 t_2^{10} + t_1^{10} t_2^{10}, \\ y_6 &= 8t_1^6 t_2^6 - 8t_1^8 t_2^6 - 8t_1^6 t_2^8 + 8t_1^8 t_2^8 + 2t_1^{10} t_2^6 - 2t_1^{10} t_2^8, \\ y_7 &= 14t_1^6 t_2^6 - 20t_1^8 t_2^6 + 5t_1^{10} t_2^6 - 16t_1^6 t_2^8 + 16t_1^8 t_2^8 \\ & \quad - 4t_1^{10} t_2^8 + 4t_1^6 t_2^{10} - 4t_1^8 t_2^{10} + t_1^{10} t_2^{10}, \\ y_8 &= 0, \quad y_9 = t_1^8 t_2^8, \end{aligned}$$

as well as

$$\begin{aligned} z_0 &= 1 - 2t_1^2 - 2t_2^2 + 4t_1^2 t_2^2, \\ z_1 &= -t_1^2 + 2t_1^4 - t_2^2 + 2t_2^4 + 6t_1^2 t_2^2 - 8t_1^4 t_2^2 \\ & \quad - 8t_1^2 t_2^4 + 8t_1^4 t_2^4, \\ z_2 &= 8 - 27t_1^2 + 22t_1^4 - 27t_2^2 + 22t_2^4 + 87t_1^2 t_2^2 \\ & \quad - 67t_1^4 t_2^2 + 2t_1^6 t_2^2 - 67t_1^2 t_2^4 + 49t_1^4 t_2^4 - 6t_1^6 t_2^4 \\ & \quad + 2t_1^2 t_2^6 - 6t_1^4 t_2^6 + 4t_1^6 t_2^6, \\ z_3 &= 14t_1^2 t_2^2 - 37t_1^4 t_2^2 + 22t_1^6 t_2^2 - 37t_1^2 t_2^4 + 92t_1^4 t_2^4 \\ & \quad - 50t_1^6 t_2^4 + 22t_1^2 t_2^6 - 50t_1^4 t_2^6 + 24t_1^6 t_2^6, \\ z_4 &= 45t_1^2 t_2^2 - 98t_1^4 t_2^2 + 48t_1^6 t_2^2 - 98t_1^2 t_2^4 + 197t_1^4 t_2^4 \\ & \quad - 90t_1^6 t_2^4 + 4t_1^8 t_2^4 + 48t_1^2 t_2^6 - 90t_1^4 t_2^6 + 46t_1^6 t_2^6 \\ & \quad - 6t_1^8 t_2^6 + 4t_1^4 t_2^8 - 6t_1^6 t_2^8 + 2t_1^8 t_2^8, \\ z_5 &= 20t_1^4 t_2^4 - 33t_1^6 t_2^4 + 12t_1^8 t_2^4 - 33t_1^2 t_2^6 + 46t_1^6 t_2^6 \\ & \quad - 14t_1^8 t_2^6 + 12t_1^4 t_2^8 - 14t_1^6 t_2^8 + 4t_1^8 t_2^8, \\ z_6 &= 24t_1^4 t_2^4 - 31t_1^6 t_2^4 + 8t_1^8 t_2^4 - 31t_1^2 t_2^6 + 33t_1^6 t_2^6 \\ & \quad - 9t_1^8 t_2^6 + 8t_1^4 t_2^8 - 9t_1^6 t_2^8 + 3t_1^8 t_2^8, \\ z_7 &= 2t_1^6 t_2^6 - t_1^8 t_2^6 - t_1^6 t_2^8, \quad z_8 = t_1^6 t_2^6. \end{aligned}$$

Appendix F: Characteristic function of $|\Psi\rangle_{DQC}$

Noticing the displacement operators $D_a(\alpha) = e^{\frac{|\alpha|^2}{2}} e^{-\alpha^* a} e^{\alpha a^\dagger}$, $D_b(\beta) = e^{\frac{|\beta|^2}{2}} e^{-\beta^* b} e^{\beta b^\dagger}$, the CF of $|\psi_{LQC}\rangle_{ab}$ can be calculated as

$$\begin{aligned} & \chi_E(\alpha, \beta) \\ &= \frac{\cosh^2 \lambda}{p_{cd} \cosh^2 r} \frac{d^8}{ds_1 ds_2 ds_3 ds_4 dh_1 dh_2 dh_3 dh_4} \\ & \quad e^{\Xi - \Lambda|\alpha|^2 + \chi_\alpha \alpha + \chi_{\alpha^*} \alpha^* - \Lambda|\beta|^2 + \chi_\beta \beta + \chi_{\beta^*} \beta^* + \eta_9(\alpha\beta + \alpha^* \beta^*)} \\ & \quad |_{(s_1, s_2, s_3, s_4, h_1, h_2, h_3, h_4)=0}, \end{aligned}$$

where I have set $\Lambda = \cosh^2 \lambda - \frac{1}{2}$ and

$$\begin{aligned}\chi_\alpha &= h_1\eta_4 + s_2\eta_2 - s_3\eta_8 - h_4\eta_6, \\ \chi_{\alpha^*} &= -s_1\eta_4 - h_2\eta_2 + h_3\eta_8 + s_4\eta_6, \\ \chi_\beta &= s_1\eta_1 + h_2\eta_3 - h_3\eta_5 - s_4\eta_7, \\ \chi_{\beta^*} &= -h_1\eta_1 - s_2\eta_3 + s_3\eta_5 + h_4\eta_7.\end{aligned}$$

Appendix G: the fidelity of QT of CVs

Considering the entangled state $|\psi_{LQC}\rangle_{ab}$ to teleport a coherent (vacuum) state and substituting $\chi_{in}(z) = \exp[-|z|^2/2]$ and $\chi_{out}(z) = \chi_{in}(z)\chi_E(z^*, z)$ into $F = \int \frac{d^2z}{\pi} \chi_{in}(-z)\chi_{out}(z)$ yields

$$F = \frac{\kappa_0}{p_{cd} \cosh^2 r} \frac{d^8}{\exp(\Pi) |_{(s_1, s_2, s_3, s_4, h_1, h_2, h_3, h_4)=0}},$$

where I have set

$$\begin{aligned}\Pi &= +\kappa_1 (s_1s_2 + h_1h_2) + \kappa_2 (s_3s_4 + h_3h_4) \\ &+ \kappa_3 (s_1s_3 + h_1h_3) + \kappa_4 (s_2s_4 + h_2h_4) \\ &- \kappa_5 (s_3h_2 + s_2h_3) - \kappa_6 (s_4h_1 + s_1h_4) \\ &+ \kappa_7s_1h_1 + \kappa_8s_2h_2 + \kappa_9s_3h_3 + \kappa_{10}s_4h_4.\end{aligned}$$

with $\kappa_0 = [2(1 - \tanh \lambda)]^{-1}$ and

$$\begin{aligned}\kappa_1 &= \kappa_0 r_1 r_2, \kappa_2 = (\kappa_0 + \frac{1}{2}) r_1 r_2 \tanh r, \\ \kappa_3 &= \frac{t_1 \sinh 2\lambda}{8\kappa_0} - \frac{\kappa_0 \tanh \lambda}{t_1} + t_1 \cosh^2 \lambda, \\ \kappa_4 &= \frac{t_2 \sinh 2\lambda}{8\kappa_0} - \frac{\kappa_0 \tanh \lambda}{t_2} + t_2 \cosh^2 \lambda \\ \kappa_5 &= \frac{\kappa_0 r_1 r_2 \tanh \lambda}{t_1}, \kappa_6 = \frac{\kappa_0 r_1 r_2 \tanh \lambda}{t_2}, \\ \kappa_7 &= \kappa_0 r_1^2, \kappa_8 = \kappa_0 r_2^2 \\ \kappa_9 &= \frac{\kappa_0 r_1^2}{t_1^2} \tanh^2 \lambda, \kappa_{10} = \frac{\kappa_0 r_2^2}{t_2^2} \tanh^2 \lambda\end{aligned}$$

Thus Eq.(17) can be obtained.

-
- [1] S. L. Braunstein and H. J. Kimble, Phys. Rev. Lett. **80**, 869 (1998).
[2] P. M. Anisimov, G.M. Raterman, A. Chiruvelli, W. N. Plick, S. D. Huver, H. Lee, and J.P. Dowling, Phys. Rev. Lett. **104**, 103602 (2010).
[3] H. J. Briegel, W. Dur, J. I. Cirac, and P. Zoller, Phys. Rev. Lett. **81**, 5932 (1998).
[4] S. L. Braunstein and H. J. Kimble, Phys. Rev. A **61**, 042302 (2000).
[5] R. E. S. Polkinghorne and T. C. Ralph, Phys. Rev. Lett. **83**, 2095 (1999).
[6] P. van Loock and S. L. Braunstein, Phys. Rev. A **61**, 010302 (1999).
[7] S. D. Bartlett, B. C. Sanders, S. L. Braunstein, and K. Nemoto, Phys. Rev. Lett. **88**, 097904 (2002).
[8] S. D. Bartlett and B. C. Sanders, Phys. Rev. Lett. **89**, 207903 (2002).
[9] J. Eisert, S. Scheel, and M. B. Plenio, Phys. Rev. Lett. **89**, 137903 (2002).
[10] J. Fiurasek, Phys. Rev. Lett. **89**, 137904 (2002).
[11] H. Nha, S. Y. Lee, S. W. Ji, and M. S. Kim, Phys. Rev. Lett. **108**, 030503 (2012).
[12] A. Kitagawa, M. Takeoka, M. Sasaki, and A. Chhefles, Phys. Rev. A **73**, 042310 (2006).
[13] S. Y. Lee, S. W. Ji, H. J. Kim, and H. Nha, Phys. Rev. A **84**, 012302 (2011).
[14] S. Y. Lee, S. W. Ji, and C. W. Lee, Phys. Rev. A **87**, 052321 (2013).
[15] C. Navarrete-Benlloch, R. Garcia-Patron, J. H. Shapiro, and N. J. Cerf, Phys. Rev. A **86**, 012328 (2012).
[16] Y. Yang and F. L. Li, Phys. Rev. A **80**, 022315 (2009).
[17] T. Opatrny, Kurizki, and D. G. Welsch, Phys. Rev. A **61**, 032302 (2000).
[18] P. T. Cochrane, T. C. Ralph, and G. J. Milburn, Phys. Rev. A **65**, 062306 (2002).
[19] F. Dell's Anno, S. De Siena, and F. Illuminati, Phys. Rep. **428**, 53 (2006).
[20] M. S. Kim, J. Phys. B: At. Mol. Opt. Phys. **41**, 133001 (2008).
[21] S. Y. Lee and H. Nha, Phys. Rev. A **85**, 043816 (2012).
[22] J. Fiurasek, S. Massar, and N. J. Cerf, Phys. Rev. A. **68**, 042325 (2003).
[23] H. Jeong, M. S. Kim, T. C. Ralph, and B. S. Ham, Phys. Rev. A. **70**, 061801 (2004).
[24] E. Bimbard, N. Jain, A. MacRae, and A. I. Lvovsky, Nature Photonics, **4**, 243 (2010).
[25] M. Dakna, T. Anhut, T. Opatrny, L. Knoll, and D. G. Welsch. Phys. Rev. A **55**, 3184 (1997).
[26] M. Dakna, L. Knoll, and D. Welsch, Opt. Commun. **145**, 309 (1997).
[27] B. M. Escher, A.T.Avelar, and B. Baseia, Phys. Rev. A **72**, 045803 (2005).
[28] M. Takeoka and M. Sasaki, Phys. Rev. A **75**, 064302 (2007).
[29] A. I. Lvovsky and J. Mlynek, Phys. Rev. Lett. **88**, 250401 (2002).
[30] T. J. Bartley, G. Donati, J. B. Spring, X. M. Jin, M. Barbieri, A. Datta, B. J. Smith, and I. A. Walmsley, Phys. Rev. A **86**, 043820 (2012).
[31] C. H. Bennett, H. J. Bernstein, S. Popescu, B. Schumacher, Phys. Rev. A **53**, 2046 (1996).
[32] S. J. van Enk, Phys. Rev. A **60**, 5095 (1999).
[33] J. Ryu, J. Lim, C. Lee, and J. Lee, J. Mod. Opt. **57**, 1550 (2010).

- [34] L. M. Duan, G. Giedke, J. I. Cirac, and P. Zoller, Phys. Rev. Lett. **84**, 2722 (2000).
- [35] R. Simon, Phys. Rev. Lett. **84**, 2726 (2000).
- [36] G. Giedke, B. Kraus, M. Lewenstein, and J. I. Cirac, Phys. Rev. Lett. **87**, 167904 (2001).
- [37] E. Shchukin and W. Vogel, Phys. Rev. Lett. **95**, 230502 (2005).
- [38] M. Hillery and M. S. Zubairy, Phys. Rev. Lett. **96**, 050503 (2006).
- [39] J. C. Garrison and R. Y. Chiao, Quantum Optics, Oxford University press, New York (2008).
- [40] P. Marian and T. A. Marian, Phys. Rev. A **74**, 042306 (2006).
- [41] A. V. Chizhov, L. Knoll, and D. G. Welsch, Phys. Rev. A **65**, 022310 (2002).
- [42] S. L. Braunstein, C. A. Fuchs, H. J. Kimble, and P. van Loock, Phys. Rev. A **64**, 022321 (2001).